# Chapter 3
# PET Imaging Innovation by DOI Detectors

Taiga Yamaya

**Abstract** Positron emission tomography (PET) plays important roles in cancer diagnosis, neuroimaging, and molecular imaging research. However potential points remain for which big improvements could be made, including spatial resolution, sensitivity, and manufacturing costs. Depth-of-interaction (DOI) measurement in the radiation sensor will be a key technology to get any significant improvement in sensitivity while maintaining high spatial resolution. We have developed four-layered DOI detectors based on our original light-sharing method. DOI measurement also has a potential to expand PET application fields because it allows for more flexible detector arrangement. As an example, we are developing the world's first, open-type PET geometry, "OpenPET," which is expected to lead to PET imaging during treatment. The DOI detector itself continues to evolve with the help of recently developed semiconductor photodetectors, often referred to as silicon photomultipliers (SiPMs). We are developing a SiPM-based DOI detector "X'tal cube" to achieve sub-mm spatial resolution, which is reaching the theoretical limitation of PET imaging. Innovation of SiPMs encourages our development of PET/MRI, which is attracting great notice in terms of smaller radiation exposure and better contract in soft tissues compared with current PET/CT.

**Keywords** PET • Depth-of-interaction • DOI • In-beam PET • Brain PET • SiPM • PET/MRI

## 3.1 Introduction

Positron emission tomography (PET) plays important roles in cancer diagnosis, neuroimaging, and molecular imaging research, but potential points remain for which big improvements could be made, including spatial resolution, sensitivity, and manufacturing costs. For example, the sensitivity of present PET scanners does not exceed 10 %. This means that more than 90 % of the gamma rays emitted from a subject are not utilized for imaging. Therefore, research on next generation PET technologies remains a hot topic worldwide.

T. Yamaya (✉)
Molecular Imaging Center, National Institute of Radiological Sciences, Chiba, Japan
e-mail: taiga@nirs.go.jp

The Imaging Physics Team at National Institute of Radiological Sciences (NIRS) has carried out basic studies on radiation detectors, data acquisition systems, image reconstruction algorithms, and data correction methods to improve image quality and quantity in nuclear medicine as well as to explore innovative systems.

A depth-of-interaction (DOI) detector, for which various methods have been studied [1–7], will be a key device to get any significant improvement in sensitivity while maintaining high spatial resolution (Fig. 3.1). In order to maintain enough detection efficiency, the scintillation crystals should be 2–3 cm long. In conventional detectors, the crystal thickness causes uncertainty in position identification, which results in degraded spatial resolution at the peripheral area of a field-of-view. On the other hand, DOI can reduce the parallax error while maintaining the efficiency.

We have developed four-layered DOI detectors based on a light-sharing method [8, 9]. One successful proof of concept was the "jPET" project, in which we developed brain prototype PET with our DOI detectors; almost uniform spatial resolution around 2 mm all over the field-of-view was obtained with iterative image reconstruction with geometrically defined system matrix [10]. We have also succeeded to upgrade the DOI detector to have better spatial resolution with cheaper production costs: successful identification of $32 \times 32 \times 4$ array of LYSO crystals sized in $1.45 \times 1.45 \times 4.5$ mm$^3$ with a 64ch flat panel PMT (H8500, Hamamatsu Photonics K.K., Japan) [11], which has enabled Shimadzu's new products of positron emission mammography.

DOI measurement also has a potential to expand PET application fields because it allows for more flexible detector arrangement. As an example, we are developing the world's first, open-type PET geometry, "OpenPET," which is expected to lead to PET imaging during treatment. In addition, flexible system design of OpenPET
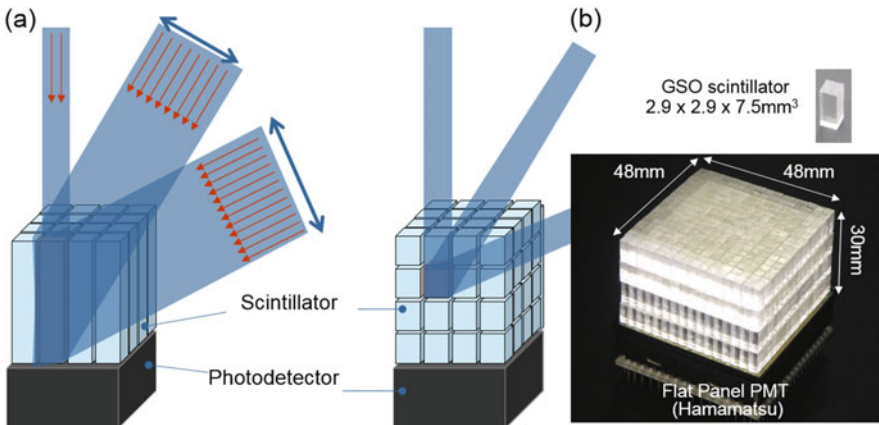


**Fig. 3.1** Comparison between a conventional PET detector (**a**) and our depth-of-interaction (DOI) detector. The DOI detector (**b**) eliminates the parallax error, which is caused by the thickness of crystals in conventional 2D detectors

prototypes is enabling us to develop an innovative brain scanner "helmet-chin PET." The DOI detector itself continues to evolve with the help of recently developed semiconductor photodetectors, often referred to as silicon photomultipliers (SiPMs). We are developing a SiPM-based DOI detector "X'tal cube" to achieve sub-mm spatial resolution, which is reaching the theoretical limitation of PET imaging. Innovation of SiPMs encourages our development of PET/MRI, which is attracting great notice in terms of smaller radiation exposure and better contract in soft tissues compared with current PET/CT. By using our SiPM-based DOI detectors, we are developing a novel, high-performance, and low-cost brain PET/MRI to meet demands for earlier diagnosis of Alzheimer's disease. The key concept is a RF coil with DOI PET detectors, which has a potential to upgrade any existing MRI to PET/MRI. In this paper, an overview of above developments is shown.

## 3.2   The OpenPET: A Future PET for Therapy Imaging

OpenPET is our original idea to realize the world's first open-type 3D PET scanner for PET-image guided particle therapy such as in situ dose verification and direct tumor tracking. The principal of dose verification for particle therapy is based on the measurement of positron emitters which are produced through fragmentation reactions caused by proton or $^{12}$C ion irradiation. Even with a full-ring geometry, the OpenPET has an open gap between its two detector rings through which the treatment beam passes, while conventional positron cameras applied to particle therapy imaging have been basically limited to planar imaging with lower detection efficiency [12–14]. Following our initial proposal of the dual-ring OpenPET (DROP) in 2008 (Fig. 3.2a) [15], we developed a small prototype in 2010 to show a proof of concept (Fig. 3.2b) [16]. In 2011, we also proposed the single-ring OpenPET (SROP), which is more efficient than DROP in terms of manufacturing cost and sensitivity [17]. We developed two small SROP prototypes in 2012 and 2013 (Fig. 3.2d, e) [18, 19], and we succeeded in visualizing a 3D distribution of beam stopping positions inside a phantom with the help of radioactive beams ($^{11}$C beam and $^{10}$C beam) used as primary beams (Fig. 3.2f) [20]. Following these good results, in 2014, we have finally developed a whole-body prototype of DROP (Fig. 3.2g) [21].

The key technology which enabled OpenPET is our original, four-layered DOI detector. In order to measure radiations from the limited activity produced though fragmentation reactions, Zr-doped GSO (GSOZ), which contains less natural radioactivity, was chosen for the scintillators instead of Lu-based scintillators although timing performance was compromised. In order to compensate for the limited light yield, on the other hand, we used 64-channel, flat-panel PMTs with a super-bialkali photocathode (Hamamatsu R10552-100-M64), which had a 30 % higher quantum efficiency [22]. In order to enable stable in-beam PET measurement even under high background radiations, voltage divider circuits were designed so as to have
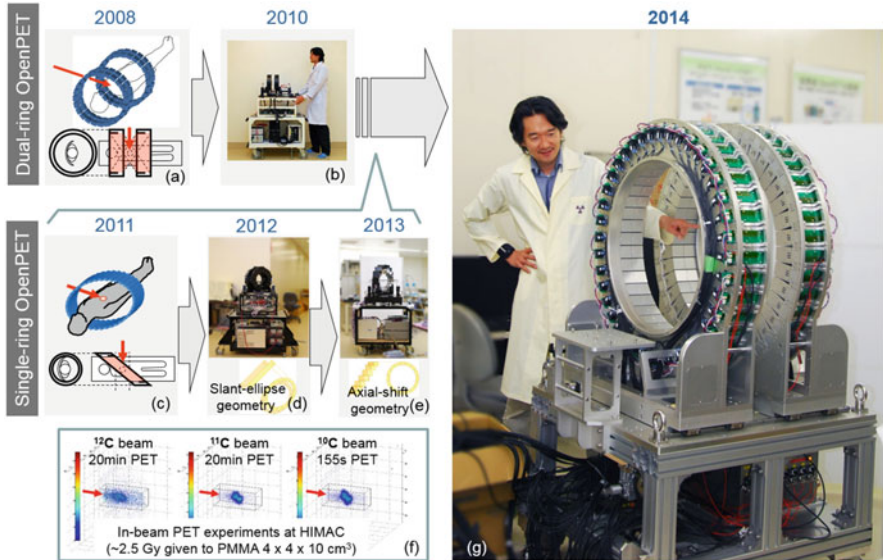
**Fig. 3.2** Conceptual sketches and prototypes of the OpenPET geometries: the dual-ring OpenPET (DROP) (**a–b**) and the single-ring OpenPET (**c–e**). Following proofs-of-concept of in-beam imaging (**f**), a whole-body DROP was developed (**g**)

five times higher linearity. In order to avoid severe radiation damage, in addition, gain control ASICs were not implemented in the front-end circuits, and position analyzer circuits were placed with a 15-m cable extension. A data acquisition system was developed based on the single events collection.

The prototype consisted of two detector rings, and each detector ring had two subrings of 40 detectors. Each detector consisted of $16 \times 16 \times 4$ array of GSOZ ($2.8 \times 2.8 \times 7.5$ mm$^3$). The portable gantry had a compact design; each detector ring had a 940 mm outer diameter and 171 mm thickness for the detector inner bore of 640 mm diameter and 113 mm thickness.

## 3.3 The Helmet-Chin PET for Super High-Sensitive Brain Imaging

For a potential demand for brain molecular imaging, prototypes of brain dedicated PET scanners have been developed. However all previous developments are based on a cylindrical geometry [3, 10, 23–25], which is not the most efficient for brain imaging. Making the detector ring as small as possible is essential in PET, because sensitivity can be increased with a limited number of detectors. With appropriate DOI detectors, which reduce the parallax error caused by the thickness of the scintillators, spatial resolution can be maintained, or even improved by reducing

the angular deviation effect. Therefore, we developed the world's first helmet-chin PET, in which DOI detectors are arranged to form a hemisphere, for compact, high-sensitivity, high-resolution, and low-cost PET imaging [26, 27].

Our basic idea relies on the evidence that the average sensitivity of a hemisphere PET is about 1.5-times higher than that of a cylinder PET of the same radius and height, while surface area is the same for both geometries (Fig. 3.3a, b). In addition, use of 12 % more detectors for "chin detectors," which are placed like a chin strap, improves sensitivity especially at the central area (Fig. 3.3c). In the prototype, 47 block detectors were used to form a hemisphere of 25 cm inner diameter and 50 cm outer diameter, and seven block detectors were used for the chin strap (Fig. 3.3d). The total number of detectors was about only 1/5 of that to be used in whole body PET. Each detector block was a four-layered DOI detector, which consisted of 1024 Zr-doped GSO crystals (2.8 mm × 2.8 mm × 7.5 mm) and a high-sensitivity type of 64-channel flat-panel PMT. The data acquisition system was
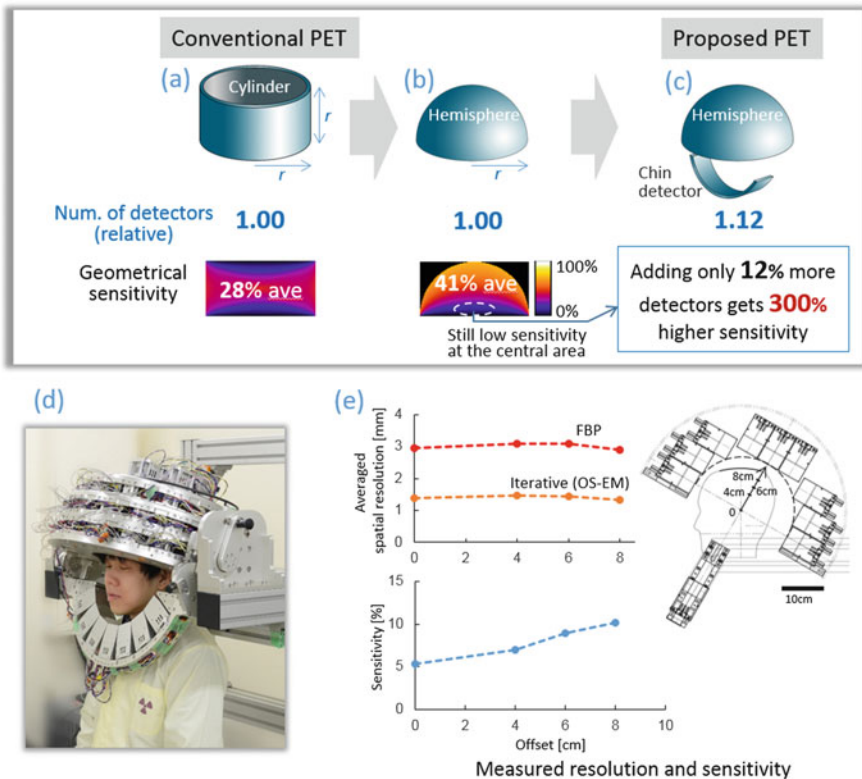


**Fig. 3.3** Comparison between a conventional cylinder PET (**a**) and the proposed helmet-chin PET (**b, c**); the hemisphere detector arrangement obtains 1.5 times higher sensitivity, and adding only 12 % more detectors gets three times higher sensitivity at the central area. A prototype of the helmet-chin PET (**d**) succeeded in obtaining excellent sensitivity and resolution performance (**e**)

developed based on single event collection. An iterative reconstruction method with detector modeling was applied.

Measured sensitivity was 5 % at the cerebellum region and 10 % at the parietal region for a standard 400–600 keV energy window. Averaged FWHM of point sources was 3.0 mm (FBP) and 1.4 mm (iterative) (Fig. 3.3e).

## 3.4 The X'tal Cube: 0.8 mm Isotropic Resolution, a World Record

X'tal (crystal) cube is a future DOI detector we are developing. SiPMs, multi-pixel photon counters (MPPCs), are coupled on all sides of a scintillation crystal block, which is segmented into a 3D array of cubes [28] (Fig. 3.4a). Crystal segmentation is made by irradiating a laser to a monolithic crystal (Fig. 3.4b) [29]. No reflector is inserted into the crystal block so that scintillation light originating in one of the cubic segment spreads 3-dimensionally and distributes among all MPPCs on the crystal block. In 2012, we achieved 1-mm cubic resolution with $18 \times 18 \times 18$ segments made by 3D laser processing (Fig. 3.4c, d) [30, 31]. In the last year, we succeeded in identifying $(0.8 \text{ mm})^3$ crystal segments, which is a world record [32].
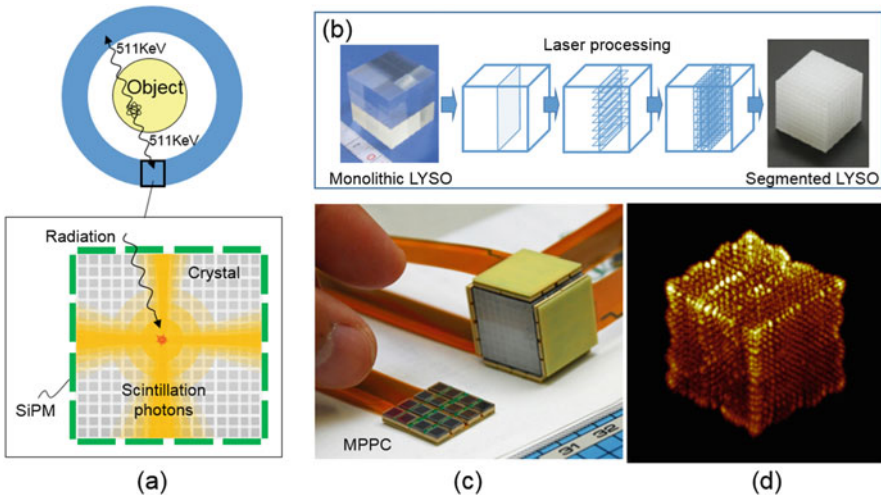


**Fig. 3.4** Conceptual sketch of the X'tal cube (**a**) and a prototype X'tal cube detector (**c**) with a monolithic crystal block segmented by the 3D laser processing (**b**). A flood histogram shows position identification performance of $18 \times 18 \times 18$ array of 1 mm$^3$ crystal segments (**d**)

## 3.5   The Add-On PET: A PET Insert to Upgrade Existing MRI to PET/MRI

One of the major innovations made in recent years is combined PET/MRI
(Fig. 3.5a) [33–46], but utilization of DOI measurement in PET detectors has not
been studied well. DOI measurement, which allows for use of a smaller detector
ring, is essential for PET in order to exploit the excellent potentials of PET imaging
in terms of improved spatial resolution and sensitivity as well as reduced production
costs of PET instrument. Therefore we proposed a new combined PET/MRI that
makes full use of DOI measurement (Fig. 3.5b) [47, 48].

In order to make a PET detector ring as small as possible while placing
electronic parts such as photodetectors and front-end circuits outside of a RF coil,
PET detector modules were placed between spokes of the birdcage RF coil
(Fig. 3.5c). For each detector module, electronic parts were covered with a Cu
shielding box with a hole in front of the photodetectors, and scintillators were
sticking out of the shielding box to allow their placement inside of the birdcage coil
(Fig. 3.5e). In theory, the proposed birdcage coil integrated with PET detectors can
be applied to any existing MRI as an additional choice of RF coils. For a proof of
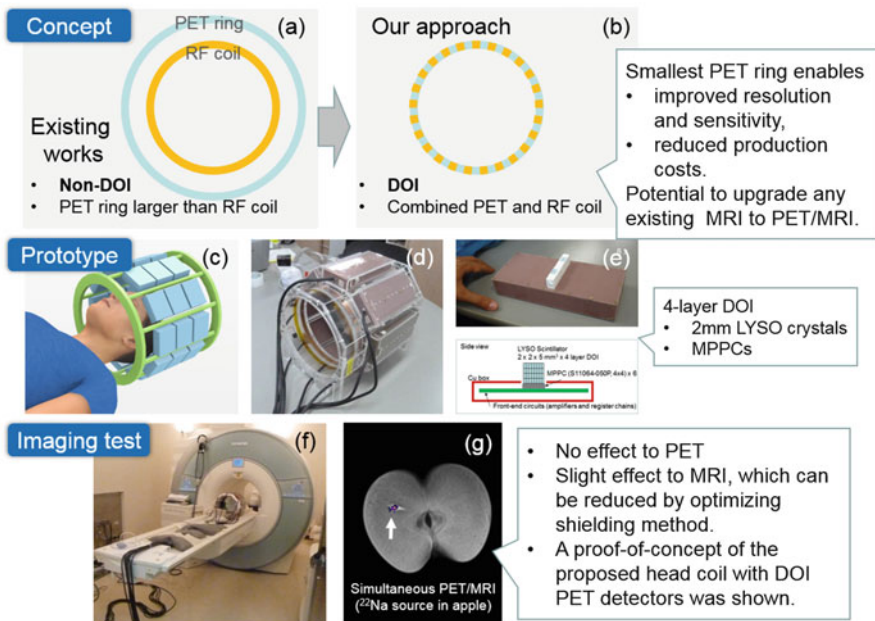


**Fig. 3.5** Concept comparison between conventional PET/MRI (**a**) and the proposed add-on
PET/MRI (**b**). A prototype (**c, d**) combined with DOI detector modules (**e**) was applied to 3T
MRI (**f**) to demonstrate simultaneous PET/MRI imaging (**g**)

concept, we developed a full-ring prototype (four-layered arrays of 2.0 mm-LYSO with MPPCs) (Fig. 3.5d), which was applied to a 3T MRI (MAGNETOM Verio, Siemens) (Fig. 3.5f).

After evaluating interference between PET and MRI, no undesirable effect was seen in the PET imaging in terms of energy resolution and position identification. While a uniform static magnetic field was obtained, about a 20 % decrease in signal-to-noise ratio was observed in MR images; we suspected this was due to noise contamination from outside the MRI room. Although further optimization is required for shielding, we demonstrated a proof of concept of the proposed head coil with DOI PET detectors (Fig. 3.5g).


## 3.6   Conclusions

In PET, DOI measurement is a key technology to get significant improvement in sensitivity while maintaining high spatial resolution. DOI measurement also has a potential to expand PET application fields because it allows for more flexible detector arrangement. In this paper, two current developments, the OpenPET toward PET-image guided particle therapy and the helmet-chin PET for high-sensitive brain imaging, were shown. Current development status of the next-generation DOI detector X'tal cube, which uses SiPMs as a photosensor, was also described. SiPM-based DOI detector enabled the add-on PET, which is a PET insert having a potential to upgrade existing MRI to PET/MRI.

# References

1. Carrier C, Martel C, Schmitt D, Leconte R. Design of a high resolution positron emission tomograph using solid state scintillation detectors. IEEE Trans Nucl Sci. 1988;35:685–90.
2. Yamamoto S, Ishibashi H. A GSO depth of interaction detector for PET. IEEE Trans Nucl Sci. 1998;45:1078–82.
3. Wienhard K, Schmand M, Casey ME, Baker K, Bao J, Eriksson L, et al. The ECAT HRRT: performance and first clinical application of the new high-resolution research tomograph. IEEE Trans Nucl Sci. 2002;49:104–10.
4. Yamashita T, Watanabe M, Shimizu K, Uchida H. High resolution block detectors for PET. IEEE Trans Nucl Sci. 1990;37:589–93.
5. Moses WW, Derenzo SE, Melcher CL, Manente RA. A room temperature LSO/PIN photodiode PET detector module that measures depth of interaction. IEEE Trans Nucl Sci. 1995;42:1085–9.
6. Miyaoka RS, Lewellen TK, Yu H, McDaniel DL. Design of a depth of interaction (DOI) PET detector module. IEEE Trans Nucl Sci. 1998;45:1069–73.
7. Shao Y, Silverman RW, Farrell R, Cirignano L, Grazioso R, Shah KS, et al. Design studies of a high resolution PET detector using APD arrays. IEEE Trans Nucl Sci. 2000;47:1051–7.
8. Murayama H, Ishibachi H, Uchida H, Omura T, Yamashita T. Depth encoding multicrystal detectors for PET. IEEE Trans Nucl Sci. 1998;45:1152–7.
9. Inadama N, Murayama H, Omura T, Yamashita T, Yamamoto S, Ishibashi H, et al. A depth of interaction detector for PET with GSO crystals doped with different amounts of Ce. IEEE Trans Nucl Sci. 2002;49:629–33.
10. Yamaya T, Yoshida E, Obi T, Ito H, Yoshikawa K, Murayama H. First human brain imaging by the jPET-D4 prototype with a pre-computed system matrix. IEEE Trans Nucl Sci. 2008;55:2482–92.
11. Tsuda T, Murayama H, Kitamura K, Yamaya T, Yoshida E, Omura T, et al. A four-layer depth of interaction detector block for small animal PET. IEEE Trans Nucl Sci. 2004;51:2537–42.
12. Pawelke J, Byars L, Enghardt W, Fromm WD, Geissel H, Hasch BG, et al. The investigation of different cameras for in-beam PET imaging. Phys Med Biol. 1996;41:279–96.
13. Iseki Y, Mizuno H, Futami Y, Tomitani T, Kanai T, Kanazawa M, Kitagawa A, Murakami T, Nishio T, Suda M. Positron camera for range verification of heavy-ion radiotherapy. Nucl Inst Methods Phys Res A. 2003;515:840–9.
14. Nishio T, Ogino T, Nomura K, Uchida H. Dose-volume delivery guided proton therapy using beam on-line PET system. Med Phys. 2006;33:4190–7.
15. Yamaya T, Inaniwa T, Minohara S, Yoshida E, Inadama N, Nishikido F, et al. A proposal of an open PET geometry. Phys Med Biol. 2008;53:757–73.
16. Yamaya T, Yoshida E, Inaniwa T, Sato S, Nakajima Y, Wakizaka H, et al. Development of a small prototype for a proof-of-concept of OpenPET imaging. Phys Med Biol. 2011;56:1123–37.
17. Tashima H, Yamaya T, Yoshida E, Kinouchi S, Watanabe M, Tanaka E. A single-ring OpenPET enabling PET imaging during radiotherapy. Phys Med Biol. 2012;57:4705–18.
18. Yoshida E, Tashima T, Wakizaka H, Nishikido F, Hirano Y, Inadama N, et al. Development of a single-ring OpenPET prototype. Nucl Inst Methods Phys Res A. 2013;729:800–8.
19. Yamaya T, Yoshida E, Tashima H, Nakajima Y, Nishikido F, Hirano Y, et al. A prototype of a novel transformable single-ring OpenPET. In: IEEE nuclear science symposium conference record. Piscataway: IEEE; 2013. M07-1.
20. Urakabe E, Kanai T, Kanazawa M, Kitagawa A, Noda K, Tomitani T, et al. Spot scanning using radioactive $^{11}$C beams for heavy-ion radiotherapy. Jpn J Appl Phys. 2001;40:2540–8.
21. Yamaya T, Yoshida E, Tashima H, Inadama N, Nishikido F, Hirano Y, et al. Whole-body dual-ring OpenPET for in-beam particle therapy imaging. In: IEEE nuclear science symposium conference record. Piscataway: IEEE; 2014. M15-8.

22. Hirano Y, Nitta M, Inadama N, Nishikido F, Yoshida E, Murayama H, et al. Performance evaluation of a depth-of-interaction detector by use of position-sensitive PMT with a super-bialkali photocathode. Radiol Phys Technol. 2014;7:57–66.

23. Yamamoto S, Honda M, Oohashi T, Shimizu K, Senda M. Development of a brain PET system, PET-Hat: a wearable PET system for brain research. IEEE Trans Nucl Sci. 2011;58:668–73.

24. Majewski S, Proffitt J, Brefczynski-Lewis J, Stolin A, Weisenberger AG, Xi W, et al. HelmetPET: a silicon photomultiplier based wearable brain imager. In: IEEE nuclear science symposium conference record. Piscataway: IEEE; 2011. p. 4030–4.

25. Omura T, Moriya T, Yamada R, Yamauchi H, Saito A, Sakai T. Development of a high-resolution four-layer DOI detector using MPPCs for brain PET. In: IEEE nuclear science symposium conference record. 2012. p. 3560–3.

26. Tashima H, Ito H, Yamaya T. A proposed helmet-PET with a jaw detector enabling high-sensitivity brain imaging. In: IEEE nuclear science symposium conference record. 2013. M11-11.

27. Yamaya T, Yoshida E, Tashima H, Inadama N, Shinaji T, Wakizaka H, et al. First prototype of a compact helmet-chin PET for high-sensitivity brain imaging. J Nucl Med. 2015;56:317.

28. Yamaya T, Mitsuhashi T, Matsumoto T, Inadama N, Nishikido F, Yoshida E, et al. A SiPM-based isotropic-3D PET detector X'tal cube with a three-dimensional array of 1 mm3 crystals. Phys Med Biol. 2011;56:6793–807.

29. Moriya T, Fukumitsu K, Sakai T, Ohsuka S, Okamoto T, Takahashi H, et al. Development of PET detectors using monolithic scintillation crystals processed with sub-surface laser engraving technique. IEEE Trans Nucl Sci. 2010;57:2455–9.

30. Yoshida E, Hirano Y, Tashima H, Inadama N, Nishikido F, Moriya T, et al. Impact of the laser-processed X'tal cube detector on PET imaging in a one-pair prototype system. IEEE Trans Nucl Sci. 2013;60:3172–80.

31. Yoshida E, Tashima H, Hirano Y, Inadama N, Nishikido F, Muraya H, et al. Spatial resolution limits for the isotropic-3D PET detector X'tal cube. Nucl Inst Methods Phys Res A. 2013;728:107–11.

32. Munetaka N, Inadama N, Hirano Y, Nishikido F, Yoshida E, Tashima H, et al. The X'tal cube PET detector of isotropic $(0.8 \text{ mm})^3$ crystal segments. In: IEEE nuclear science symposium conference record. 2014. M04-1.

33. Shao Y, Cherry S. Simultaneous PET and MR imaging. Phys Med Biol. 1997;42:1965–70.

34. Slates RB, Farahani K, Shao Y, Marsden PK, Taylor J, Summers PE, et al. A study of artefacts in simultaneous PET and MR imaging using a prototype MR compatible PET scanner. Phys Med Biol. 1999;44:2015–27.

35. Catana C, Wu Y, Judenhofer MS, Qi J, Pichler BJ, Cherry SR. Simultaneous acquisition of multislice PET and MR images: initial results with a MR-compatible PET scanner. J Nucl Med. 2006;47:1968–76.

36. Pichler BJ, Judenhofer MS, Catana C, Walton JH, Kneilling M, Nutt RE, et al. Performance test of an LSO-APD detector in a 7-T MRI scanner for simultaneous PET/MRI. J Nucl Med. 2006;47:639–47.

37. Schlyer D, Vaska P, Tomasi D, Woody C, Maramraju S-H, Southekal S, et al. A simultaneous PET/MRI scanner based on RatCAP in small animals. In: IEEE nuclear science symposium conference record. 2007. p. 3256.

38. Schlemmer HP, Pichler BJ, Schmand M, Burbar Z, Michel C, Ladebeck R, et al. Simultaneous MR/PET imaging of the human brain: feasibility study. Radiology. 2008;248:1028–35.

39. Yamamoto S, Hatazawa J, Imaizumi M, Shimosegawa E, Aoki M, Sugiyama E, et al. A multi-slice dual layer MR-compatible animal PET system. IEEE Trans Nucl Sci. 2009;56:2706–13.

40. Yamamoto S, Imaizumi M, Kanai Y, Tatsumi M, Aoki M, Sugiyama E, et al. Design and performance from an integrated PET/MRI system for small animals. Ann Nucl Med. 2010;24:89–98.

41. Kwon SI, Lee JS, Yoon HS, Ito M, Ko GB, Choi JY, et al. Development of small-animal PET prototype using silicon photomultiplier (SiPM): initial results of phantom and animal imaging studies. J Nucl Med. 2011;52:572–9.
42. Maramraju SH, Smith SD, Junnarkar SS, Schulz D, Stoll S, Ravindranath B, et al. Small animal simultaneous PET/MRI: initial experiences in a 9.4 T microMRI. Phys Med Biol. 2011;56:2459–80.
43. Zaidi H, Ojha N, Morich M, Griesmer J, Hu Z, Maniawski P, et al. Design and performance evaluation of a whole-body ingenuity TF PET-MRI system. Phys Med Biol. 2011;56:3091–106.
44. Delso G, Fürst S, Jakoby B, Ladebeck R, Ganter C, Nekolla SG, et al. Performance measurements of the Siemens mMR integrated whole-body PET/MR scanner. J Nucl Med. 2011;52:1914–22.
45. Yoon HS, Ko GB, Kwon SI, Lee CM, Ito M, Chan Song I, et al. Initial results of simultaneous PET/MRI experiments with an MRI-compatible silicon photomultiplier PET scanner. J Nucl Med. 2012;53:608–14.
46. Lee B J, Grant A M, Chang C-M, Levin C S. MRI measurements in the presence of a RF-penetrable PET insert for simultaneous PET/MRI. Abstract Book of 2015 World Molecular Imaging Congress. 2015. SS 126.
47. Nishikido F, Obata T, Shimizu K, Suga M, Inadama N, Tachibana A, et al. Feasibility of a brain-dedicated PET-MRI system using four-layer detectors integrated with an RF head coil. Nucl Instr Methods A. 2014;756:6–13.
48. Nishikido F, Tachibana A, Obata T, Inadama N, Yoshida E, Suga M, et al. Development of 1.45-mm resolution four-layer DOI–PET detector for simultaneous measurement in 3T MRI. Radiol Phys Technol. 2015;8:111–9.